Bulletin of the Geological Society of Finland, Vol. 95, 2023, pp 83–106 https://doi.org/10.17741/bgsf/95.2.001

New age constraints for metasedimentary rocks in southern Finland

Paula E. Salminen[1*] and Matti Kurhila[1]

[1] *Geological Survey of Finland, Vuorimiehentie 5, FI-02151 Espoo, Finland*

VERTAISARVIOITU
KOLLEGIALT GRANSKAD
PEER-REVIEWED
www.tsv.fi/tunnus

Abstract

Metasedimentary rocks from nine sampling sites in southern Finland and an intermediate dyke in one of these sites were sampled for analysis of U–Pb zircon age and geochemical composition. The zircons of the metasedimentary rock samples yield $^{207}Pb/^{206}Pb$ dates ranging from 3281 to 1810 Ma. The nearly concordant dates from apparent detrital zircon cores indicate a prominent source with age around 2.1–2.0 Ga. The maximum depositional ages estimated for six of the metasedimentary rock samples span from 1.96 to 1.89 Ga. The data from zircon rims and overgrowths and metamorphic zircons in the metasedimentary rock samples indicate regional metamorphic events in the study area at least at ca. 1.89 and 1.84 Ga, and possibly also at ca. 1.87 Ga. The minimum age of the deposition (≤1.89 Ga) was estimated based on the ages of the regional metamorphism and the intrusive rocks. Some zircon rims and overgrowths yield ≥1.91 Ga $^{207}Pb/^{206}Pb$ dates, which are considered to possibly represent metamorphic events in the source areas.

Keywords: Zircon, U–Pb zircon age, maximum depositional age, metamorphic age, detrital, Palaeoproterozoic

* Corresponding author (e-mail: paula.salminen@gtk.fi)

Editorial handling: Jarmo Kohonen (email: jarmo.kohonen@helsinki.fi)

1. Introduction and geological setting

The depositional age of sedimentary rocks can be constrained as a time span between the minimum and maximum age. The minimum age is typically defined by the dated cross-cutting/overlying geological units or by overprinting features, such as metamorphic minerals. The maximum age can be obtained by dating stratigraphically underlying rock units or fragments (clasts) in the sedimentary rock. Accordingly, age determination of single detrital zircons can be used in the assessment of the source rocks but also in estimation of the maximum depositional age of a sedimentary rock unit (e.g., Fedo et al. 2003; Zimmerman et al. 2018).

Dating of detrital zircon grains is a commonly used method in evaluation of the maximum depositional age (MDA), the estimated oldest possible age for the rock. However, reliable MDA results are complicated to obtain. Several methods to define the MDA have been proposed, and many sources of bias must be considered. The MDA can be based, for example, youngest detrital zircon, youngest graphical peak, youngest age cluster or some algorithm (see e.g., Coutts et al. 2019; Vermeesch 2021). Depending on the applied method, the obtained MDAs may be too old or young, and better precision can be achieved with a larger dataset (Coutts et al. 2019; see also Andersen 2005). Discordance and lead loss cause biases in detrital zircon geochronology (e.g., Spencer et al. 2016; Andersen et al. 2019). Other sources of bias include common lead correction (e.g., Andersen et al. 2019) and sampling error (e.g., Fedo et al. 2003; Andersen et al. 2018a, 2018b).

Regarding the provenance, it must be noted that detrital zircons only register those source components which include zircons (e.g., Andersen et al. 2019). In addition, detrital grains may be recycled, even multiple times (e.g., Andersen et al. 2018a) in sedimentary systems, and the primary source (e.g., sedimentary rock) may be different from the ultimate igneous source of the zircon grains. Furthermore, the metamorphic zircon growth may occur after the deposition of the sediment (see e.g., Rasmussen 2005; Dhuime et al. 2007; Mikkola et al. 2018a), and some zircons may have been entirely recrystallised and reset for their U-Pb system during metamorphism (e.g., Nelson 2001; Kohn & Kelly 2018). Therefore, zircon rims and overgrowths may represent post-depositional growth and they commonly yield younger ages than the respective core domains (see e.g., Zimmerman et al. 2018).

The present study area is located in southern (S-SW) Finland (Fig. 1), and the aim of our study is to provide additional age constraints based on dated zircons in the metasedimentary rocks deposited and metamorphosed during the Svecofennian orogeny (ca. 1.92–1.79 Ga; see e.g., Lahtinen et al. 2005 and references therein). According to Johansson et al. (2022), early Svecofennian magmatism would have begun already at ca. 1.95 Ga, and there was a major peak between 1.90 and 1.85 Ga, and younger major peak at 1.8 Ga. In S-SW Finland, metasedimentary rocks are often found in association with metavolcanic rocks yielding ages between 1.90–1.86 Ga (e.g., Reinikainen 2001; Väisänen & Mänttäri 2002; Skyttä et al. 2005; Pajunen et al. 2008; Väisänen & Kirkland 2008; Nironen & Mänttäri 2012; Kara et al. 2020). The plutonic rocks in S-SW Finland include ca. 1.89–1.87 Ga felsic and mafic intrusions (e.g., Huhma 1986; Patchett & Kouvo 1986; Väisänen et al. 2002; Nironen et al. 2016; Kara et al. 2020, 2021) and ca. 1.86–1.81 Ga granites (e.g., Huhma 1986; Kurhila et al. 2005; Skyttä & Mänttäri 2008; Kurhila et al. 2011) intruding and migmatising the supracrustal rocks. Accordingly, the study area is also known as the late Svecofennian granite–migmatite zone of southern Finland (Ehlers et al. 1993).

The southernmost Finland has been divided into the Häme and Uusimaa belts (Fig. 1b) dominated by metavolcanic and metasedimentary rocks, respectively (e.g., Lahtinen et al. 2005; Nironen 2017a). A major part of the metasedimentary rocks of southern Finland belongs to either the Häme migmatite suite or the Kimito suite (Fig. 1b). The samples of this study were collected from both suites to bring up the potential age difference. In addition, we wanted to collect samples from different types of metasedimentary rocks.

The metasedimentary rocks from nine sampling sites (Fig. 1b) were analysed for U–Pb zircon age and geochemical composition. As a result, we provide estimates of the maximum depositional ages for six samples. We also estimate the age of the metamorphism and use these metamorphic ages in constraining the minimum age of the studied metasedimentary rocks. The absolute minimum age of the deposition was obtained by dating one cross-cutting dyke sample in one of the sampling sites. Additionally, the obtained whole-rock geochemical data provide support for the speculations concerning the protolith, provenance and tectonic setting of the sampled metasedimentary rocks.

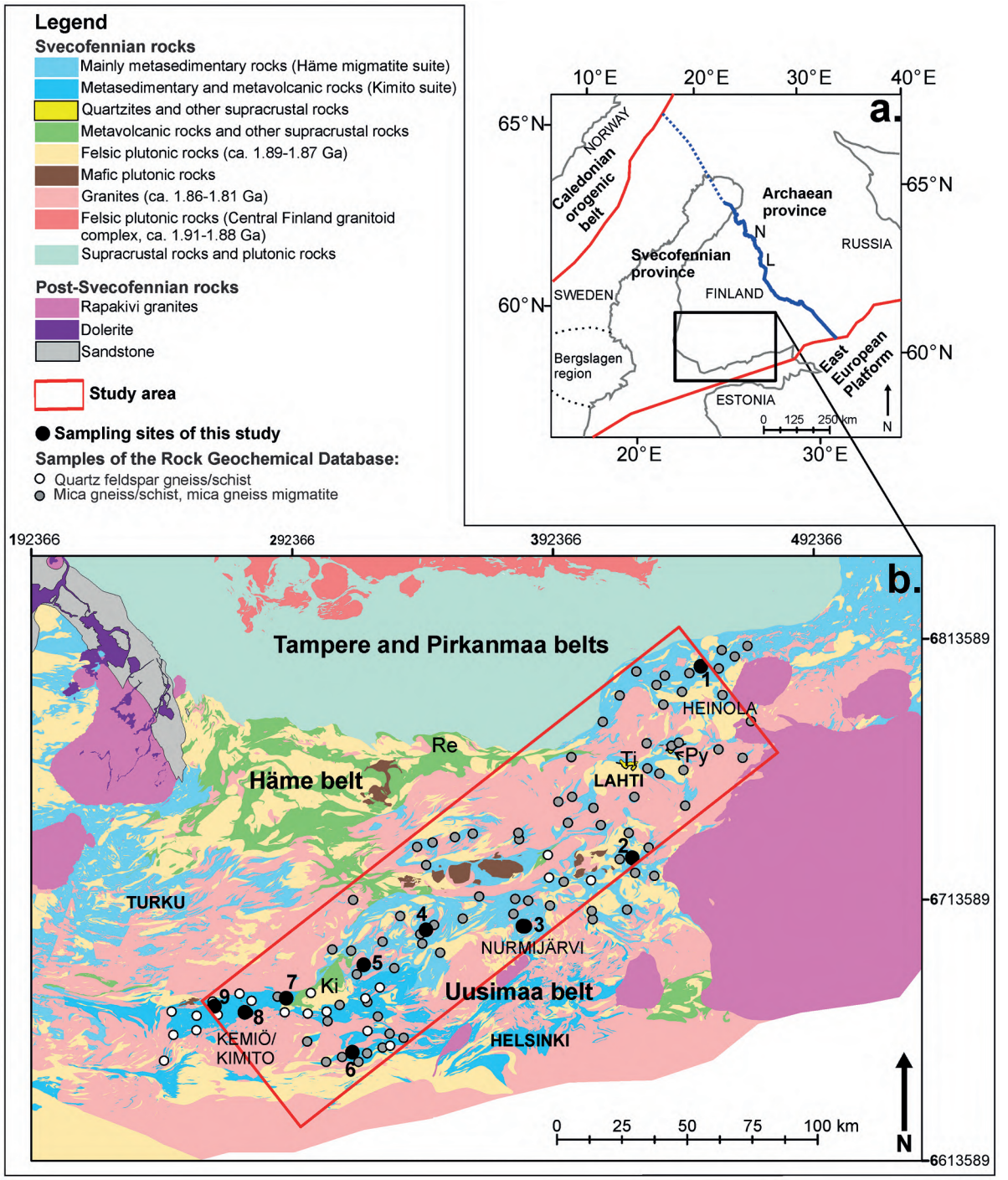

Figure 1. (a) A schematic map showing the location of figure b, the boundaries of the Fennoscandian shield (red line), the Raahe-Ladoga cryptic suture separating the Svecofennian and Archean crustal provinces (solid blue line, blue dotted line in postulated NW part), the location of the Bergslagen region (black dotted line) and approximate locations of the Näläntöjärvi suite (N) and Lampaanjärvi suite (L). (b) A simplified geological map of the southern (S-SW) Finland, modified from Bedrock of Finland scale free (2022). The study area and the sampling sites are indicated on the map. The abbreviations: Ki = Kisko group, Ti = Tiirismaa suite in Tiirismaa area, Py = Pyhäntaka formation, Re = Renkajärvi suite. Locations of samples from Rock Geochemical Database of Finland (Rasilainen et al. 2007) that were used for comparison are also indicated.

2. Age of regional metamorphism and metasedimentary rocks in the Svecofennian province of Finland

2.1. Regional metamorphism of Svecofennian rocks in Finland

The potential effects and age of regional metamorphism are key issues in the interpretation of detrital zircon age data. The Svecofennian rocks in southern Finland have experienced medium to high-grade metamorphism, and in the study area the metamorphic grade varies from amphibolite to granulite facies (Hölttä & Heilimo 2017). The published zircon and monazite age data have been interpreted to indicate at least two metamorphic events in the Svecofennian province in Finland: one at ca. 1.89–1.86 Ga (e.g., Mouri et al. 1999; Rutland et al. 2004; Lahtinen et al. 2009, 2017; Mikkola et al. 2018b; Hölttä et al. 2019; Salminen et al. 2022) and another at ca. 1.84–1.81 Ga (e.g., Korsman et al. 1984; Mouri et al. 2005; Väisänen et al. 2002; Nironen & Mänttäri 2012; Hölttä et al. 2019; Salminen et al. 2022). Monazite ages also indicate an age peak at ca. 1.80–1.77 Ga (e.g., Hölttä et al. 2019; Salminen et al. 2022), which was interpreted to be possibly linked to a shield-wide exhumation stage (Salminen et al. 2022). Based on data from central and western Finland, older metamorphic events in the Svecofennian province have also been suggested, at ca. 1.92 Ga (e.g., Rutland et al. 2004; Williams et al. 2008; Lahtinen et al. 2009, 2017) and at ≥1.98 Ga (Rutland et al. 2004; Williams et al. 2008). Salminen et al. (2022) also reported monazite ages of ≥1.91 Ga from SE Finland, but their interpretation (detrital vs. regional metamorphic) remained open.

2.2. Age constraints for the metasedimentary rocks in the Svecofennian province in Finland

The published $^{207}Pb/^{206}Pb$ zircon dates from the metasedimentary rocks are mostly between 3.60 and 1.75 Ga from the entire Svecofennian province in Finland, and the presented MDA estimates span from ca. 1.99 to 1.84 Ga. The reported minimum ages for the Svecofennian metasedimentary rocks in Finland vary between 1.90 Ga–1.81 Ga and are mainly based on the ages of the adjacent metavolcanic or plutonic rocks (e.g., Lahtinen et al. 2002). Thus, the maximum depositional ages and minimum ages constrain the deposition of the Svecofennian metasedimentary rocks in Finland between ca. 1.99 and 1.81 Ga. A remarkable feature is that detrital zircon data from metasedimentary rocks display a major peak at ca. 2.0 Ga without any known source area of voluminous rocks of corresponding age (Huhma et al. 2011). In the following, we summarise the spread of the published U-Pb ($^{207}Pb/^{206}Pb$) zircon dates and estimated maximum depositional ages (MDAs) separately for central/western Finland, SE Finland and S-SW Finland.

In central and western Finland, the published $^{207}Pb/^{206}Pb$ zircon dates from metasedimentary rocks span from 3.60 to 1.82 Ga (Kouvo & Tilton 1966; Matisto 1968; Nironen 1989; Huhma et al. 1991; Claesson et al. 1993; Kähkönen & Huhma 1993; Alviola et al. 2001; Lahtinen et al. 2002; Rutland et al. 2004; Williams et al. 2008; Lahtinen et al. 2009; Suikkanen et al. 2014; Lahtinen et al. 2015; Kotilainen et al. 2016; Lahtinen et al. 2017; Mikkola et al. 2018b, 2018c). These data include also dates from samples from the Tampere and Pirkanmaa belts (for the location, see Fig. 1b). The presented MDAs from that area span from ca. 1.99 to 1.88 Ga (Lahtinen et al. 2002; Rutland et al. 2004; Williams et al. 2008; Lahtinen et al. 2009, 2015; Kotilainen et al. 2016; Lahtinen

et al. 2017; Mikkola et al. 2018b, 2018c). These MDA estimates were based on youngest detrital zircon age (Kotilainen et al. 2016), the youngest age cluster/group of detrital zircons (Lahtinen et al. 2002; Williams et al. 2008; Lahtinen et al. 2009, 2015, 2017; Mikkola et al. 2018b, 2018c), and in the case of Rutland et al (2004) the youngest detrital zircon cores or a pre-depositional metamorphic event. Mikkola et al. (2018b) and Williams et al. (2008) also took in account the metamorphic ages in evaluation of the MDAs.

In SE Finland, the published $^{207}Pb/^{206}Pb$ zircon dates from metasedimentary rocks mostly span from 3.38 to 1.75 Ma (Korsman et al. 1984, 1988; Vaasjoki & Sakko 1988; Lahtinen et al. 2002; Bergman et al. 2008; Mikkola et al. 2018b; Lahtinen et al. 2022). Korsman et al. (1984) considered that all of their analysed zircons (with $^{207}Pb/^{206}Pb$ dates from 1846 to 1780 Ma) represent metamorphic crystallisation. The published MDAs for the metasedimentary rocks in SE Finland span from ≥1.93 to 1.84 Ga (Lahtinen et al. 2002; Bergman et al. 2008; Mikkola et al. 2018b; Lahtinen et al. 2022). These MDAs were based on the youngest zircon (Bergman et al. 2008), the youngest age cluster/group of detrital zircons (Lahtinen et al. 2002), the youngest age peak of detrital zircons in a probability density plot (Lahtinen et al. 2022), and in the case of Mikkola et al. (2018b) either based on the youngest cluster or the youngest "bulk" age. A rather reliable MDA is locally provided by the postulated upper intercept age (1885 ± 6 Ma) for the granitoid cobbles in the Haukivuori (Hepojärvi) conglomerate (Korsman et al. 1988).

In S-SW Finland, the published detrital zircon studies represent rather small areas and are based on a small total number of samples (13 samples), and only few grains were analysed from three of those samples. Also, most of the previously provided MDAs from S-SW Finland were based on samples collected from a small area in the northeastern part of our study area. As a result, the knowledge regarding the depositional age of these metamorphic rock units is limited. Excepting a few younger dates, other published $^{207}Pb/^{206}Pb$ zircon dates from metasedimentary rock samples from S-SW Finland, from our study area or slightly outside of it, span from 3.32 to 1.79 Ga (Hopgood et al. 1983; van Duin 1992; Claesson et al. 1993; Lahtinen et al. 2002; Väisänen et al. 2002; Bergman et al. 2008; Nironen & Mänttäri, 2012; Lahtinen et al. 2017, 2022). The data of van Duin (1992; one sample within the Häme migmatite suite) are strongly discordant and yield an Archaean upper intercept age.

The published MDAs from our study area span from ca. 1.90 to 1.85 Ga. The MDAs for the quartzites of *the Tiirismaa suite* in the Tiirismaa ("Ti" in Fig. 1b) and Hyvinkää areas, have been reported as 1.87–1.85 Ga (Lahtinen et al. 2002; Bergman et al. 2008). Bergman et al. (2008) provided an MDA of 1.87 Ga for the quartzites of *the Pyhäntaka formation* ("Py" in Fig. 1b). Nironen & Mänttäri (2012) reported maximum depositional ages of ca. 1.89–1.87 Ga for the cordierite paragneisses within *the Häme migmatite suite*. These cordierite paragneisses are found in the Pyhäntaka area but they are stratigraphically distinct from the Pyhäntaka formation. Lahtinen et al. (2022) estimated a maximum depositional age of 1.87 Ga for felsic volcano-sedimentary gneiss in the Hämeenlinna area, within *the Häme migmatite suite*. Claesson et al. (1993) stated that ca. 2.1 Ga zircons were prominently present in a metagreywacke sample of the *Kisko group (*"Ki" in Fig. 1b), and Lahtinen et al. (2022) considered the maximum depositional age of 1.90 Ga as most probable for this same sample. In addition, Lahtinen et al. (2017) provided a maximum depositional age of 1.92 Ga for a psammitic metasedimentary rock sample of *the Renkajärvi suite* ("Re" in Fig. 1b), slightly outside of our study area. These MDA estimates were based on the youngest zircon (Bergman et al. 2008), the youngest age cluster/group of detrital zircons (Lahtinen et al. 2002, 2017), or the youngest age peak of detrital zircons in a probability density plot (Lahtinen et al. 2022). Nironen & Mänttäri (2012)

defined the MDAs based on the mean age of the youngest U–Pb dates from zircons, which show magmatic compositional zoning, but they also reported the MDA estimates based on the youngest single ages.

Torvela & Kurhila (2022) provided age constraints for gneisses (pyroxene granulites) in the Vihti area, southern Finland. They were collected close to the sampling sites 3 and 4 of this study. The mineralogy of these rocks was described to vary from "clinopyroxene-rich tonalitic gneisses to Ca-rich, scapolite-clinopyroxene-calcite gneisses with an unknown protolith". Torvela & Kurhila (2022) reported $^{207}Pb/^{206}Pb$ zircon dates of ca. 3.4–1.79 Ga and protolith ages of ca. 1908, 1911 and 1946 Ma from these rocks.

3. Sampling sites and characterisation of the samples

The analysed samples were collected from nine sampling sites (SS = sampling site/sites; Fig. 1b, Fig. 2, Table 1). For convenience, the samples are mostly referred to by the number of the sampling site, but sometimes also the age determination ID (A-number). Some information of the sampled rocks and their geochemical features is given below. Further information and data are provided in Electronic Appendices. A more detailed description of the sampling sites and samples can be found in Appendix A, the description of the methodology for the geochemical analyses in Appendix B, and the geochemical data and some Harker diagrams in Appendix C. The zircons extracted from the samples are described in Appendix A and zircon images can be found in Appendix D.

Table 1. Sampling sites (SS = sampling site, HMS = Häme migmatite suite, KS = Kimito suite, Sample field code = the internal sample field code of Geological Survey of Finland).

SS	Locality	Coordinates (Euref: N, E)	Unit	Sample field code	Age determination ID	Lithology	Comments
1	Heinola	6802998, 449081	HMS	PESA-2020-27.1	A2568	Biotite paragneiss	
2	Orimattila	6729677, 422854	HMS	PESA-2020-30.1	A2569	Biotite paraschist	No zircons could be extracted from the sample.
3	Nurmijärvi	6703355, 380833	HMS	PESA-2020-31.1	A2570	Garnet-bearing paragneiss	The rock is in a contact with microcline granite. The sample includes some leucosome and pegmatite.
			–	PESA-2020-31.2	A2571	Intermediate dyke	The dyke is crosscutting microcline granite. The sample includes lighter coloured patches.
4	Vihti	6702108, 343678	HMS	PESA-2020-38.1	A2577	Pyroxene-biotite paragneiss	The rock is a diatexite and it has a rusty weathering surface. The rock is in contact with microcline granite.
5	Lohja	6688629, 319841	HMS	PESA-2020-37.1	A2576	Pyroxene-quartz-feldspar paragneiss	
6	Raasepori	6655175, 315536	KS	PESA-2020-35.1	A2574	Biotite paragneiss	The sample includes some leucosome and one layer-parallel vein of pegmatite.
7	Salo	6675880, 290159	KS	PESA-2020-36.1	A2575	Biotite paraschist	
8	Särkisalo, Kemiö	6670358, 274311	KS	PESA-2020-32.1	A2572	Quartz-feldspar paraschist	Only 1 zircon was extracted from the sample. The rock has a rusty weathering surface.
9	Kemiö	6672786, 262617	KS	PESA-2020-34.1	A2573	Quartz-feldspar paragneiss	Only 6 zircons were extracted from the sample

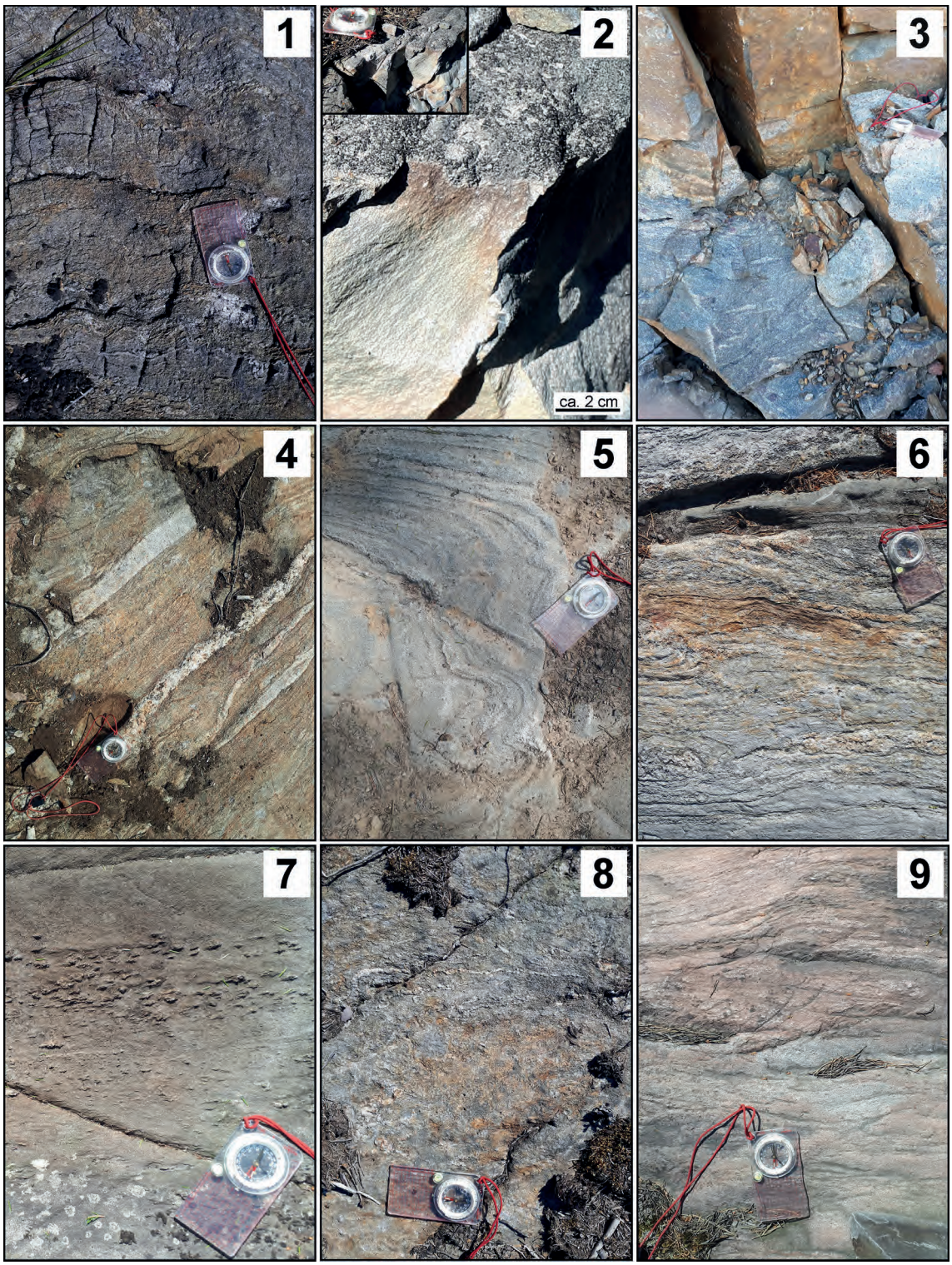

Figure 2. Selected photos of the studied outcrops labelled by the sampling site numbers. The length of the compass is ca. 11.5 cm. The compass is pointing approximately northwards in each photo (note the scale and inset photo in the case of the sampling site 2). Photos: Paula Salminen/Geological Survey of Finland (GTK).

The metasedimentary rocks of SS 1–5 represent the Häme migmatite suite. Sampling sites 1 and 2 are located in middle amphibolite facies areas and SS 3–5 within a granulite facies area (see Hölttä & Heilimo 2017). The SiO_2 contents of the metasedimentary rocks from the Häme migmatite suite span from ca. 56 to 73 wt.%. They mainly yield Al_2O_3 contents of ca. 12–16 wt.%, but the garnet-bearing paragneiss sample from SS 3 has a higher Al_2O_3 content (ca. 20 wt.%). The sample from SS 1, the northernmost of the sampling sites, represents biotite paragneiss with layered appearance (Fig. 2). The compositional variation plausibly represents pelitic and psammitic layers in the gneissose rock. The sample has a rather high SiO_2 content (72.53 wt.%). The sample from SS 2 represents biotite paraschist. No zircons could be extracted from this sample. Two samples were collected from SS 3: a sample from a garnet-bearing paragneiss and a sample from an intermediate dyke (SiO_2 52.54 wt.%). The dyke crosscuts a microcline granite at the same outcrop. Based on the field observations, the granite is younger than the paragneiss. The paragneiss sample includes some leucosome and pegmatite. The sampled rock at SS 4 was interpreted as a paragneiss. It is referred to as pyroxene-biotite paragneiss. In the field, this rock appears as a diatexite. It has a rusty weathering surface. It is in contact with microcline granite. The paragneiss sample from this site is enriched in Fe_2O_3 (12.32 wt.%) and MgO (5.58 wt.%), but it is unclear whether this is because of a mafic source (also Cr 270 ppm) or because of a restite origin. The sample from SS 5 is referred to pyroxene-quartz-feldspar paragneiss. At the sampling site, that rock is gneissose and layered. This calc-silicate-bearing rock is rich in CaO (8.88 wt.%) and it probably contained a sedimentary carbonate component before metamorphism. Accordingly, the siliciclastic component of the protolith would have had a higher SiO_2 content than that of the paragneiss (65.29 wt.%). This rock locally includes feldspar grains/clasts (1–3 mm in diameter) of uncertain origin.

Sampling sites 6–9 are located within the Kimito suite. SS 6 and 8 represents high amphibolite facies and SS 7 and 9 low amphibolite facies rocks (see Hölttä & Heilimo 2017). The samples from the Kimito suite include ca. 60–84 wt.% of SiO_2 and ca. 8–16 wt.% of Al_2O_3. The sample from SS 6 is from a biotite paragneiss, including some leucosome and one thin (ca. 1–2 cm) layer-parallel pegmate vein. In the field, the paragneiss is migmatitic/gneissose and layered. The high SiO_2 content (83.52 wt.%) points to a high amount of quartz in the protolith. The sampled rock at SS 7 represents biotite paraschist. In the field, it shows faint layering. The sample from SS 8 is referred as quartz-feldspar paraschist. Only one zircon was extracted from this sample. In the field, this rock has a rusty weathering surface. The sampled rock includes sulphides and the sample shows high Cu, Pb and Zn contents. The sample from SS 9 represents quartz-feldspar paragneiss. Only six zircons were extracted from this sample. In the field, this rock shows faint layering. This rock locally includes apparent larger feldspar grains of uncertain origin.

4. Isotope analytical methods

Age determinations and the preparation and imaging of samples for the analyses were performed in the laboratories of the Geological Survey of Finland (GTK), Espoo, Finland. Extraction of zircons from the samples was done by crushing, sieving, heavy liquid separation and magnetic separation. The process is described in detail in Appendix B. Magnetic separation was only used when the heavy mineral yield was high. Magnetic separation was not done for samples A2569, A2572, A2573 and A2575, from which every zircon grain was extracted for analysis. From the other samples, a selection of various types of zircons, representative of their abundances in each sample, was hand-picked from the heavy non-magnetic fraction. Back-scattered electron (BSE) and cathodoluminescence

(CL) images were taken from selected zircons using SEM. Both types of images were used in targeting the analysis spots.

The samples were analysed using an LA–SC–ICP–MS (laser ablation single collector inductively coupled plasma mass spectrometry) instrument composed of a Nu Plasma AttoM single collector ICP-MS connected to a Photon Machine Excite 193nM ArF laser ablation system. The analytical procedure is described Appendix B. During the LA–SC–ICP–MS analyses, Th and U contents were measured based on the respective compositions of the standard sample GJ1. According to Piazolo et al. (2017), GJ1 is chemically exceptionally homogeneous. We only used Th/U ratios ($^{232}Th/^{238}U$) to evaluate, whether a certain date might represent e.g., a metamorphic age. Isotope ratios were calculated from the raw data with the software Saturn (Silva et al. 2023). The U-Pb isotope data were plotted, and the ages were calculated using the Isoplot/Ex 4.15 software (Ludwig 2012). All ages are reported with 2σ errors and without decay constant errors.

5. Age results

In this article, *nearly concordant* refers to analyses that are <10 % normally or reversely discordant and $^{206}Pb_c$ <2 %. Thus, a few analyses, which are <10 % discordant but show $^{206}Pb_c \geq 2$ % were also filtered out from the nearly concordant dataset.

5.1. LA–SC–ICP–MS results for dyke A2571

All LA–SC–ICP–MS data from the dyke can be found in Appendix D. The analysed zircons from the intermediate dyke yield $^{207}Pb/^{206}Pb$ dates from 1891 to 1791 Ma. The spread of $^{207}Pb/^{206}Pb$ dates is relatively similar for the nearly concordant data, from 1891 to 1808 Ma. Th/U values for the analyses from the dyke are 0.18–0.69. Most of the grains show zoning, although not always concentric. Duplicate (two) analyses were obtained from some of the grains and their different zones. In most cases, the differences between the $^{207}Pb/^{206}Pb$ dates from the duplicate analyses of the same grain are within the 2σ errors. It appears that the different zones are of approximately the same age.

In the case of grain 26, the two analyses from different zones yield an age difference slightly exceeding the 2σ error limits. However, the younger $^{207}Pb/^{206}Pb$ date is more discordant (10 % above concordia) than the older date (7 % above concordia). Thus, the different zones may in this case represent growth zones of approximately the same age, but the zone with the younger date may also represent, for example, younger metamorphic growth. In the case of grain 69, the age difference between the spots clearly exceeds the 2σ error limits. The older and younger domain yield $^{207}Pb/^{206}Pb$ dates of 1891 and 1835 Ma, respectively, and both analyses are nearly concordant. The older domain may represent a xenocrystic core, as its date is the oldest of all the dates from the dyke. The younger date probably represents a rim/overgrowth, either representing the metamorphic age or the age of crystallisation of the dyke.

The nearly concordant analyses from the dyke yield an upper intercept age of 1846 ± 6 Ma (Fig. 3a). The weighted mean age ($^{207}Pb/^{206}Pb$ dates) for these data is 1843 ± 5 Ma (Fig. 3b). Only one analysis from each grain was taken into account in the calculation of these ages; the more discordant analysis was omitted. In the case of grain 69, the analysis from the rim/overgrowth was included in the calculations, but the analysis from the possibly xenocrystic core (also the more discordant analysis) was omitted. A concordia plot for all data from the dyke can be found in Appendix D.

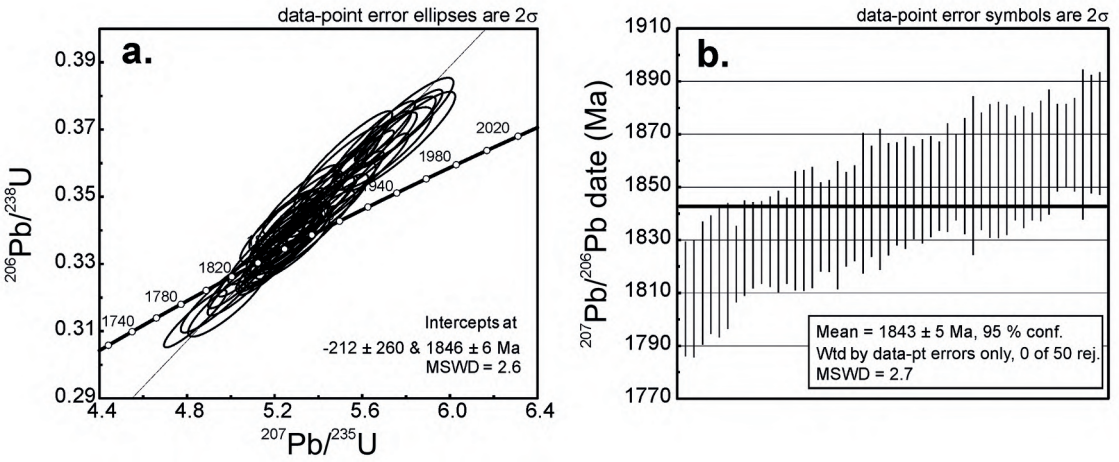

Figure 3. The age of the intermediate dyke at the sampling site 3 (sample A2571): (a) the upper intercept age based on nearly concordant data and (b) the weighted mean age based on nearly concordant data. Nearly concordant refers to analyses that are <10 % normally or reversely discordant and have $^{206}Pb_c$ <2 %. In the case of duplicate analyses from a certain grain, only the less discordant analysis was included in the calculations and the plots (see also subsection 5.1).

5.2. LA–SC–ICP–MS results for the metasedimentary rocks

All LA–SC–ICP–MS data for the metasedimentary rocks can be found in Appendix D and the results for these are summarised in Table 2. No zircons were found from sample A2569 (SS 2), while only one zircon was extracted from sample A2572 (SS 8), and its analysis yielded an invalid result. Five zircons were analysed from sample A2573 (SS 9), but most of the analyses are discordant. Only two nearly concordant analyses were obtained from this sample, yielding $^{207}Pb/^{206}Pb$ dates of 1890 Ma (grain 4) and 2089 Ma (grain 6).

The metasedimentary rocks from the sampling sites 1 and 3–7 (A2568/SS 1, A2570/SS 3, A2577/SS 4, A2576/SS 5, A2574/SS 6, A2575/SS 7) yield $^{207}Pb/^{206}Pb$ dates from 3281 to 1810 Ma (Fig. 4a, b). The spread of $^{207}Pb/^{206}Pb$ dates is similar for the nearly concordant data and for all data. The nearly concordant data from each of the sampling sites display a relatively continuous spread for $^{207}Pb/^{206}Pb$ dates ≤2230 Ma (Fig. 4c–h). The concordia plots for each sample can be found in Appendix D.

One analysis (spot c) from grain 26 in sample A2568 was targeted at an apparent rim, but it is located at the border of two zones and it possibly yields a mixed age. The younger analysis (1911 Ma) from the outer part of the grain 60 in sample A2574 yields a very high Th/U ratio (2.31), while the older analysis (1990 Ma) from the inner domain of this grain yields a low Th/U ratio (0.04). In addition, the $^{206}Pb_c$ (%) for this younger date is higher (ca. 1.9) than that for the older date (ca. 0.0). So, it is not clear what these two dates actually represent (e.g., a core or an overgrowth).

The analysed zircons (except the grain 60 of sample A2574) have an apparent core and at least one rim/overgrowth, but the rim is sometimes only weakly visible. Occasionally, the core domains show internal zoning. Table 2 presents the spread on per-sample basis the $^{207}Pb/^{206}Pb$ dates from the zircon core domains and the $^{207}Pb/^{206}Pb$ dates for the rims/overgrowths.

Most of the core domains were interpreted as detrital ones. All data from the detrital zircon cores, including duplicate analyses from some cores, yield $^{207}Pb/^{206}Pb$ dates from 3281 to 1810 Ma. The spread of nearly concordant dates from these cores is similar,

Table 2. Summary of the age data for the metasedimentary rock samples (SS = sampling site). The maximum depositional ages are based on nearly concordant analyses (for details, see subsection 6.2.). Nearly concordant refers to analyses that are less than 10 % discordant (normally or reversely) and have $^{206}Pb_c$ <2 %. Below, zircon cores refer to apparent detrital core domains if not otherwise mentioned.

SS	Age determination ID (lithology)	Number of analysed zircons	Number of analysed spots	Spread of $^{207}Pb/^{206}Pb$ dates (Ma)				Interpreted maximum depositional age	Comments
				All data	Nearly concordant data	Zircon cores (all dates)	Rims and overgrowths (all dates)		
1	**A2568** (biotite paragneiss)	53	62	2889–1883	2889–1883	2889–1883 (n = 55, duplicate analyses from two grains)	2187, 2071, 2029. 1930, 1913, 1891	1.89 Ga (n = 4)	One analysis yield a possibly mixed age (1971 Ma) between the core and the rim.
2	**A2569** (biotite paraschist)	No zircons were extracted from the sample							
3	**A2570** (garnet-bearing paragneiss)	49	59	2973–1838	2948–1838	Detrital cores: 2973–1866 (n=46, duplicate analyses from grain 84) Metamorphic grains: 1880–1838 (n = 4)	1959, 1958. 1943, 1891, 1867, 1864, 1860, 1844, 1839	1.93 Ga (n = 6)	
4	**A2577** (pyroxene-biotite paragneiss)	47	51	2642–1810	2642–1810	2642–1810 (n = 48, duplicate analyses from grain 50)	1951, 1896, 1825	1.91 Ga (n = 4)	
5	**A2576** (pyroxene-quartz-feldspar paragneiss)	36	47	3144–1823	3144–1832	3144–1835 (n = 37, duplicate analyses from grains 9 and 12)	2035, 1996, 1914, 1912. 1876, 1844, 1841, 1835 1832, 1823	1.90 Ga (n = 3)	
6	**A2574** (biotite paragneiss)	48	54	3281–1896	3281–1896	3281–1896 (n = 50, duplicate analyses from three grains)	1985, 1980	1.96 Ga (n = 2)	Two analyses (1990 and 1911 Ma) from grain 60 are not listed in the dates for cores, rims and overgrowths; see section 5.2
7	**A2575** (biotite paraschist)	25	26	2810–1904	2810–1904	2810–1904 (n = 26, duplicate analyses from grain 17)	No rims/ overgrowths were analysed	1.91 Ma (n = 2)	
8	**A2572** (quartz-feldspar paraschist)	1	1	The analysis yield an invalid result.					
9	**A2573** (quartz-feldspar paragneiss)	5	7	2089–1846	Only two nearly concordant analyses: 2089, 1890	2089–1846 Ma (n = 7, duplicate analyses from grains 3 and 5)	No rims/ overgrowths were analysed	Not determined (only two nearly concordant analyses)	

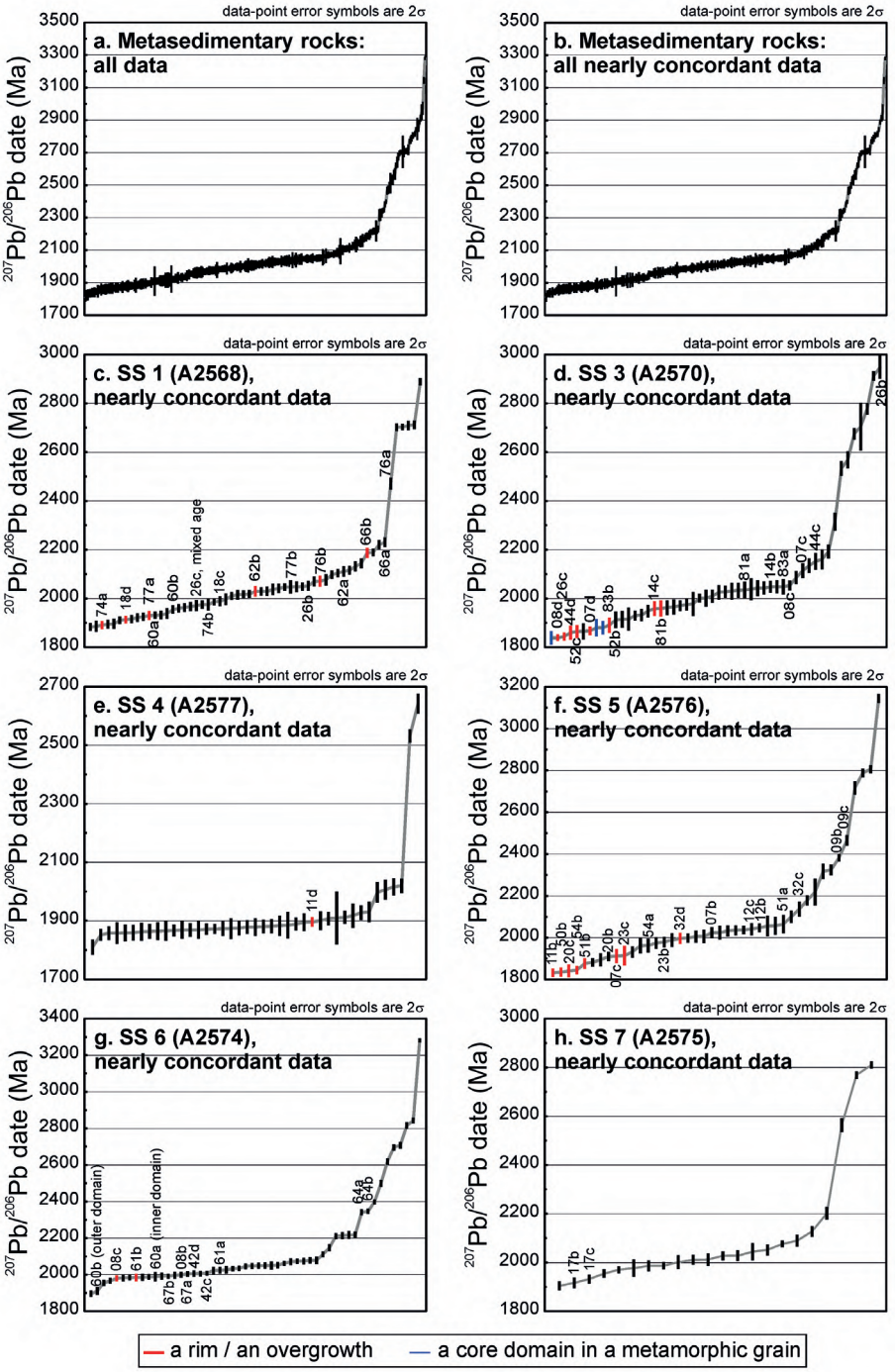

Figure 4. Metasedimentary rocks: the spread of $^{207}Pb/^{206}Pb$ dates for (a) all data, (b) all nearly concordant analyses and (c–h) nearly concordant analyses from the sampling sites 1 and 3–7 (SS = sampling site). Nearly concordant refers to analyses that are <10 % normally or reversely discordant and have $^{206}Pb_c$ <2 %. The dataset includes two analyses from some of the zircons (from different zones of the core or one from the core and the other from the rim/overgrowth); these have been marked in the images c–g. In a few cases, this dataset does not include the analysis from the core, but the analysis from the rim/overgrowth is still marked in the images. No zircons were extracted from the sample of SS 2, and the analysis of the only extracted zircon from the sample of SS 8 was invalid. Only two nearly concordant analyses were obtained from the sample of SS 9 (see Table 2).

but two of the three <1.85 Ga dates are discordant. Th/U ratios for these detrital zircon cores were mostly >0.20 (242/269 analyses) but show a total spread from these was from 0.01 to 1.70.

In the case of five grains, the $^{207}Pb/^{206}Pb$ dates from duplicate analyses from apparent detrital core domains yield an age difference exceeding the 2σ error limits. These age differences between the two analyses from the same core domain might be explained by different discordances of the spots. In one case (grain 84/A2570), the older analysis also shows elevated common lead content ($^{206}Pb_c$ 5.0 %).

Four grains from the sample A2570 (SS 3) with weakly visible rim were interpreted as metamorphic grains: the analyses from their core domains yield low Th/U ratios (0.01–0.04) and relatively young $^{207}Pb/^{206}Pb$ dates (1880–1838 Ma).

Apparent rims and overgrowths of the grains yield $^{207}Pb/^{206}Pb$ dates that are younger (age difference >2σ error limits) than those from the respective core domains. The data from rims and overgrowths yield $^{207}Pb/^{206}Pb$ dates of 1896–1823 Ma (n = 15), 1959–1912 Ma (n = 8), 1980 Ma, 1985 Ma, 1996 Ma, 2029 Ma, 2035 Ma, 2071 Ma and 2187 Ma. The single analysis from grain 11 of sample A2576 is also interpreted to represent a rim/overgrowth, because it was obtained from the outer part of the grain, and it yields a young $^{207}Pb/^{206}Pb$ date (1832 Ma) and a low Th/U ratio (0.09). The analyses from rims/overgrowths show Th/U ratios from 0.00 to 0.51; mostly <0.20 (22/30 analyses).

6. Discussion

6.1. Discordance

Some of the obtained analyses were normally or reversely discordant (for the determination of the discordance in this study, see Appendix B). In general, normal discordance can be explained by the loss of radiogenic lead, Gain of excess uranium or incorporation of common lead (e.g., Mezger & Krogstad 1997; Andersen et al. 2019). Reverse discordance is more difficult to explain. In this study, it results probably from analytical issues (e.g., effects from different matrices between the calibration standard and unknowns), taking into account that the reference samples also sometimes showed reverse discordance. To correct for the matrix effect, we used a secondary standard (see Appendix B).

6.2. Maximum depositional ages

Despite the challenges of the detrital zircon geochronology, discussed in section 1, we present MDA estimates based on the youngest robust age peaks in probability density plots (Fig. 5). Basically, our aim is: (1) to provide constraints for the depositional age (the MDA estimate vs. the minimum age), and (2) to provide data for comparison to the previous MDA estimates. The presented MDA estimates are based on at least two nearly concordant $^{207}Pb/^{206}Pb$ dates from apparent detrital zircon cores. When duplicate analyses from a certain core were available, only the less discordant analysis was included in the probability density plot of the respective sampling site. The probability density plots were made by summing the probability distribution for the data with normally-distributed errors (for details, see Ludwig 2012); the plots were constructed using the $^{207}Pb/^{206}Pb$ ages and their respective analytical 2σ errors. No concordia or upper intercept ages were calculated for the age peaks, as they would have been mostly based on few analyses only and probably would not be any more reliable than the modes of the age peaks.

The estimation of the MDAs based on the youngest peak in a probability density plot may yield too old MDAs (e.g., Coutts et al. 2019), but we still considered the method more appropriate and reliable than relying on a single analysis. We also evaluated the significance of the nearly concordant dates (from detrital cores, rims/overgrowths or metamorphic grains) younger than the estimated MDA. In principle, data from rims or overgrowths and apparent metamorphic grains record post-depositional metamorphic events and were not used in the estimation of the MDAs. However, some of the rims, overgrowths or metamorphic grains

may also record pre-depositional metamorphic events.

It was not possible to estimate maximum depositional ages for the sampling sites 2, 8 or 9: no zircons could be extracted from the sample from SS 2, the only analysis from SS 8 yielded an invalid result, and only two nearly concordant analyses were obtained from SS 9. However, the youngest nearly concordant date from SS 9, from a core domain in a detrital grain, may point to deposition at ca. 1.89 Ga.

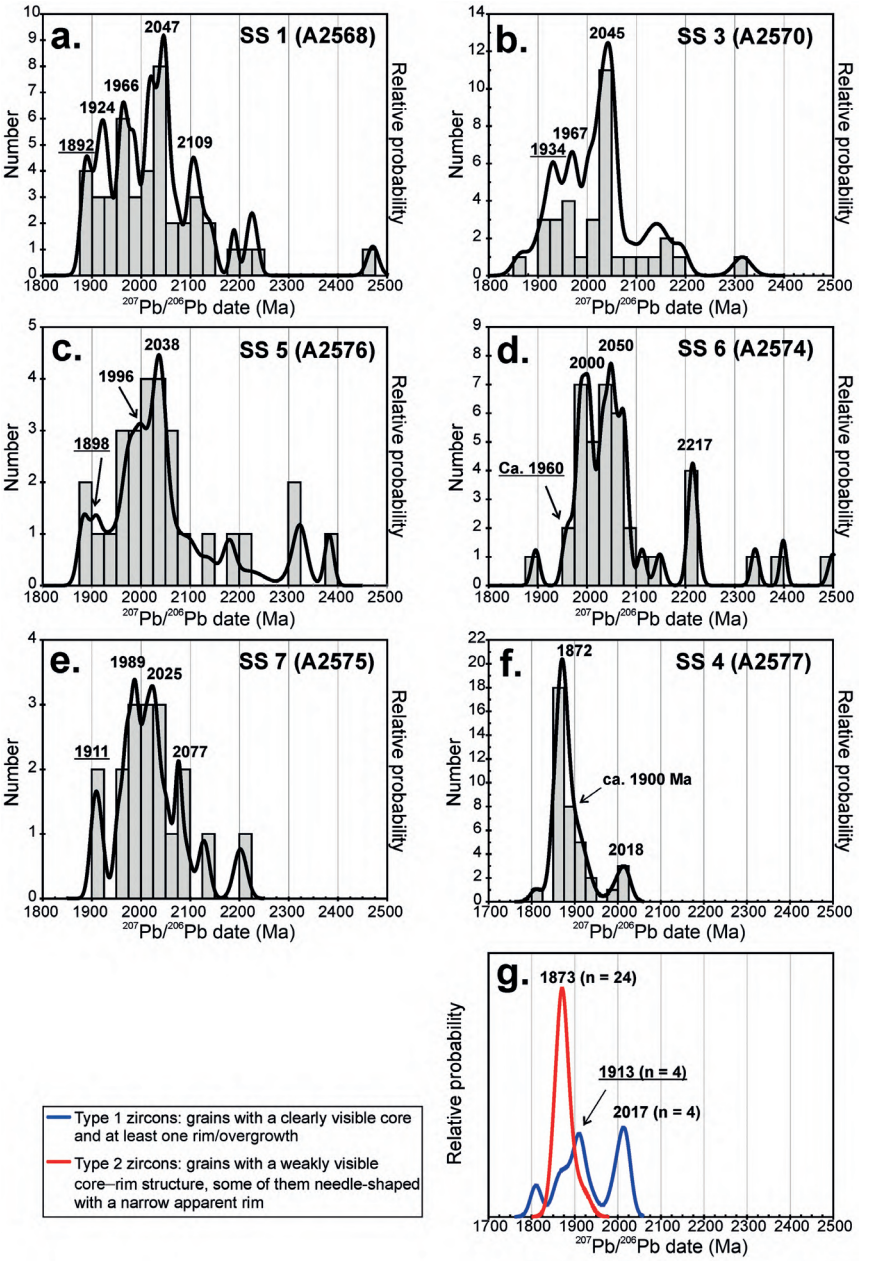

Figure 5. Metasedimentary rocks (SS = sampling site): probability density plots for nearly concordant (<10 % normally or reversely discordant and $^{206}Pb_c$ <2 %) Palaeoproterozoic $^{207}Pb/^{206}Pb$ dates from apparent detrital zircon cores: (a–f) the sampling sites 1 and 3–7, and (g) the data from SS 4 presented separately for two types of zircons. If there were duplicate analyses from some zircon core, only the less discordant one is included in the respective plot. Ages have been marked for the age peaks used for the estimation of the maximum depositional ages (ages underlined) and the most prominent age peaks of each site.

The best estimate for the MDA of SS 1 (A2568) is 1.89 Ga (Fig. 5a). One nearly concordant date from an overgrowth in that sample is also ca. 1.89 Ga, which could indicate metamorphism soon after the deposition of the rock.

SS 3–5 are within high-grade metamorphic area, and their isotopic system may have been partially or totally reset during the metamorphism (see e.g., Mezger & Krogstad 1997). However, the youngest age peak of at least two analyses of detrital zircon cores from SS 3 (A2570) indicates a relatively old maximum depositional age of 1.93 Ga (Fig. 5b). A younger date (1866 Ma) was obtained from a core domain of a grain, which appears somewhat patchy in a cathodoluminescence image: that grain has probably experienced dissolution–reprecipitation and its primary isotopic composition may have been altered in at least some patches (e.g., Mezger & Krogstad 1997). The rims, overgrowths and apparent metamorphic grains in the sample A2570 also yield nearly concordant dates younger than 1.93 Ga, but they are likely indicative of post-depositional metamorphic events (see subsection 6.3).

The data for all zircon core domains from SS 4 (A2577) form a prominent peak at ca. 1.87 Ga (Fig. 5f), which however does not probably represent the maximum depositional age of that sampling site. There are different types of zircon grains in this sample: (1) zircon grains with a clearly visible core (often with internal zoning) and at least one rim/overgrowth and (2) zircon grains with a weakly visible core–rim structure, of which some are needle-shaped with a narrow apparent rim. Type 2 grains still show the youngest age peak at ca. 1.87 Ga (Fig. 5g). This age probably records a post-depositional metamorphic age, and the needle-shaped zircons have probably grown from the melt phase during migmatisation at that time. Instead, type 1 grains display the youngest reliable peak at ca. 1.91 Ga (Fig. 5g). There are also a few younger type 1 grains, but their isotopic composition may have not been retained as they appear patchy, metamict or notably fractured. The age of 1.91 Ga is considered as the best MDA estimate for SS 4.

The best estimate for the MDA of SS 5 (A2576) is 1.90 Ga by the mode for a composite peak at ca. 1.91–1.89 Ga (Fig. 5c). The younger nearly concordant dates from rims/overgrowths (ca. 1.88–1.83 Ga) are considered to represent post-depositional metamorphic events (see subsection 6.3). One date of ca. 1.88 Ga from rims/overgrowths may indicate a metamorphic event soon after the deposition.

The age of 1.96 Ga (Fig. 5d) is considered as the best estimate of the MDA for SS 6 (A2574), based on a side peak of a larger peak (at ca. 2.00 Ga). One date (1896 Ma; Th/U = 0.01) younger than 1.96 Ga was obtained from grain 66, which appears dissolute and patchy, and therefore may not record the original isotopic composition (e.g., Mezger & Krogstad 1997). One of the two analyses from grain 60 also yields a nearly concordant date (1911 Ma) younger than 1.96 Ga, but due to its very high Th/U ratio of 2.31 it might represent fluid-mediated growth (see subsection 6.3); it also shows somewhat elevated $^{206}Pb_c$ (1.9 %).

The age of 1.91 Ga (Fig. 5e) is the best estimate for the maximum depositional age of SS 7 (A2575). No dates younger than 1904 Ma were obtained from the sample A2575; no rims/overgrowths were analysed from this sample.

Based on the estimated maximum depositional ages (MDAs), the sediments of SS 1, 4 and 5 (Häme migmatite suite) and SS 7 (Kimito suite) were deposited during the main phase of the Svecofennian orogeny. The MDAs for the sediments of SS 6 (Kimito suite) and SS 3 (Häme migmatite suite), 1.96 Ga and 1.93 Ga respectively, suggest deposition before the onset of the Svecofennian orogeny.

6.3. Metamorphic ages and minimum ages of the deposition

We evaluate the regional metamorphic ages and metamorphic ages of the source areas based on the nearly concordant data from zircon rims/overgrowths and metamorphic zircons in the metasedimentary rock samples. Rims and

overgrowths in the metasedimentary rock samples yield younger dates than those from the respective core domains, with an age difference of more than the 2σ error. These rims and overgrowths may represent metamorphic growth (e.g., Kohn & Kelly 2018). In this study, the rims, overgrowths and metamorphic grains typically show low Th/U ratios, mostly <0.20, while the apparent detrital core zones mainly show Th/U ratios of >0.20. In general, igneous zircons display high (>0.5) Th/U ratios and metamorphic zircons typically display Th/U ratios of <0.1 (Kohn & Kelly 2018, and references therein). However, this is not always the case. For example, fluid-meditated growth may also cause high Th/U ratios (see Kohn & Kelly 2018), which could perhaps also explain the high Th/U ratio (2.31) obtained from the grain 60 of sample A2574.

A half (13/25) of the nearly concordant $^{207}Pb/^{206}Pb$ dates from rims and overgrowths are ca. 1.90–1.83 Ga (Fig. 6a). The nearly concordant data from rims and overgrowths display clear age peaks at ca. 1.84 Ga and at ca. 1.89 Ga (Fig. 6b). The age peak of 1.84 Ga is based on six analyses from the granulite area (SS 3 and 5). The age peak of 1.89 Ga is based on three analyses from the granulite area (SS 3–5) and one analysis from SS 1, which is found in a middle amphibolite area. The upper intercept ages for these peaks are 1841 ± 9 Ma and 1891 ± 10 Ma, respectively (Fig. 6c, d). A slightly less prominent age peak is found at ca. 1.87 Ga (Fig. 6b), based on three nearly concordant analyses from SS 3. The age span of 1.90–1.83 Ga and the three age peaks are approximately within the suggested age span of the regional metamorphic events, at

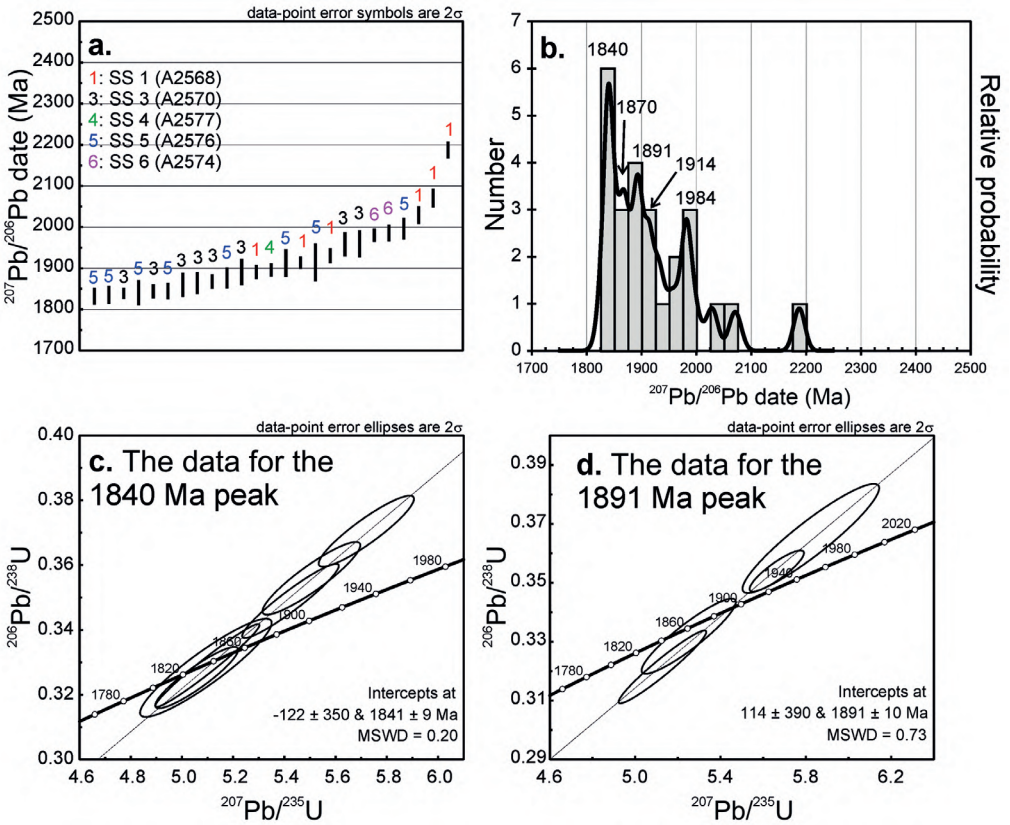

Figure 6. The rims and overgrowths of the zircons of the metasedimentary rock samples: (a) the spread of the nearly concordant $^{207}Pb/^{206}Pb$ dates (SS = sampling site), (b) the probability density plot for the nearly concordant $^{207}Pb/^{206}Pb$ dates, and (c–d) concordia plots for the two most prominent age peaks based on nearly concordant analyses. Nearly concordant refers to analyses that are <10 % normally or reversely discordant and have $^{206}Pb_c$ <2 %.

1.89–1.86 Ga (e.g., Mouri et al. 1999; Rutland et al. 2004; Lahtinen et al. 2009, 2017; Mikkola et al. 2018b; Hölttä et al. 2019; Salminen et al. 2022) and 1.84–1.81 Ga (e.g., Korsman et al. 1984; Mouri et al. 2005; Väisänen et al. 2002; Nironen & Mänttäri 2012; Hölttä et al. 2019; Salminen et al. 2022), in the Svecofennian province in Finland.

The above mentioned 1.87 Ga peak may also record the age of the migmatisation and granite emplacement, because the metasedimentary rock of SS 3 has been intruded and migmatised by microcline granite. That idea is supported by the results from SS 4, where the metasedimentary rock is also found at the contact with granite: type 2 grains (with a weakly visible core–rim structure and needle-shaped grains with a narrow apparent rim) from SS 4 also show an age peak at ca. 1.87 Ga (Fig. 5g). The ages of the microcline granites in S-SW Finland are typically ca. 1.86–1.81 Ga (e.g., Huhma 1986; Kurhila et al. 2005; Skyttä & Mänttäri 2008; Kurhila et al. 2011), and the age of 1.87 Ga is older than typical ages of the microcline granites. The granites at SS 3 or 4 were not dated in this study. However, the dyke at SS 3 was dated as ca. 1846 Ma old (Fig. 3a), and it crosscuts a microcline granite at this sampling site. The five youngest nearly concordant dates (1864–1838 Ma) from rims/overgrowths and metamorphic grains in the paragneiss sample from this sampling site are within their 2σ error limits similar to the age of the dyke.

Four zircons of sample A2570 from SS 3 are interpreted as metamorphic grains. They show dates (nearly concordant $^{207}Pb/^{206}Pb$ dates of 1880, 1879 and 1838 Ma, and a reversely discordant date of ca. 1.86 Ga), which are aligned with the dates from the rims/overgrowths in that sample and they are also within the suggested age spans of the regional metamorphic events.

The nearly concordant data from rims and overgrowths additionally yield older $^{207}Pb/^{206}Pb$ dates of ca. 2.19–1.91 Ga (n = 12; Fig. 6a), which might also be linked to metamorphic events. These dates show two age peaks of at least two analyses at 1984 Ma (n = 3) and 1914 Ma (n = 3) (Fig. 6b). Most of these 2.19–1.91 Ga dates predate the estimated maximum depositional age of the respective sampling site, which means that they may represent metamorphic events in the provenance areas. Salminen et al. (2022) reported 1.91 Ga monazite dates from SE Finland and speculated that they may have had a detrital or a metamorphic origin. Based on samples from central to western Finland, metamorphic events at >1.91 Ga have also been suggested by Rutland et al. (2004), Williams et al. (2008) and Lahtinen et al. (2009, 2017). The timing of metamorphic events at SS 2 or 7–9 cannot be evaluated. No rims/overgrowths or metamorphic grains were analysed from SS 7 or 9. The only analysis from SS 8 yielded an invalid result and no zircons were extracted from the sample from SS 2.

The minimum age of the deposition for the metasedimentary rocks can be estimated based on the age of the regional metamorphism and the ages of intrusive rocks. The rims/overgrowths of SS 1 and 3–5 record the oldest, ca. 1.89 Ga, metamorphic peak, suggesting that the minimum age of the deposition for these sites would be ca. 1.89 Ga. The sample from SS 6 yield one date of 1897 Ma from a zircon core, which appeared dissolute and patchy and can also possibly record the ca. 1.89 Ga metamorphism. Taking into account the ages of the plutonic rocks in S-SW Finland, from ca. 1.89 to 1.81 Ga (see section 1) and the previously published constraints for the oldest regional metamorphic event (ca. 1.89–1.86 Ga), the minimum age of the deposition for all studied metasedimentary rocks can be constrained to be ≤1.89 Ga. The upper intercept age (1846 ± 6 Ma) of the intermediate dyke at SS 3 provides an ultimate minimum age of the deposition for this site, and possibly also for all studied metasedimentary rocks.

In the case of SS 1 and 5, the metamorphism at 1.89 Ga would have occurred soon after the deposition. However, the depositional ages and the $^{207}Pb/^{206}Pb$ dates from the rims/overgrowths from these sites have a precision of some tens of Ma, so the actual age difference cannot be determined exactly. It cannot be either ruled out that the primary isotopic composition of the youngest detrital

grains from these two sites has been reset after the deposition.

6.4. Comparisons to other age studies in the Svecofennian province

The obtained spread of $^{207}Pb/^{206}Pb$ dates is relatively similar to the published spread of $^{207}Pb/^{206}Pb$ dates from the metasedimentary rocks in Svecofennian province in Finland (see subsection 2.2). The estimated MDAs of this study, from ca. 1.96 to 1.89 Ga, are older or similar than the previous MDA estimates from our study area (≤1.90 Ga; see subsection 2.2). The MDAs of SS 3 (1.93 Ga), SS 4 (1.91 Ga) and SS 7 (1.91) are also rather similar to the reported MDA of 1.92 Ga for the sample from the Renkajärvi suite (Lahtinen et al. 2017), in the vicinity of our study area. In addition, the protolith ages reported by Torvela & Kurhila (2022) are also close to the suggested MDAs of nearby SS 3 and SS 4.

The obtained MDAs are in the range of those reported for metasedimentary rocks in other parts of Svecofennian province in Finland (see subsection 2.2). The MDAs defined in our study are also in the range of the MDAs (1.97–1.89 Ga), which Lahtinen et al. (2015) defined for the Näläntöjärvi and Lampaanjärvi suites ("N" and "L" in Fig. 1a, respectively). The rocks of these suites have been considered to represent a Svecofennian allochtonous, tectonically displaced rocks juxtaposed across the cryptic suture on top of Archaean rocks (see Luukas & Kohonen 2021).

Lahtinen et al. (2005) considered that the Uusimaa belt may be correlative with the Bergslagen region of Sweden (Fig. 1a). This correlation between the Bergslagen region and southern parts of Finland was also already made by e.g., Allen et al. (1996). However, it should be noted that in Sweden, direct correlation of Palaeoproterozoic rocks of southern Finland to the Bergslagen region and the existence of the Bergslagen microcontinent are not favoured (e.g., Stephens & Andersson 2015). According to Stephens et al. (2009), the Bergslagen region in central Sweden is dominated by ca. 1.9–1.8 Ga Palaeoproterozoic rocks. The published $^{207}Pb/^{206}Pb$ zircon dates from metasedimentary rocks in the Bergslagen region span from ca. 2.97 to 1.83 Ga (Claesson et al. 1993, Stephens & Anderson 2015; Johansson & Stephens 2017; Kathol et al. 2020). Kuipers et al. (2018) constrained a conglomerate within the Bergslagen region as ca. 1895 Ma old, based on the U-Pb zircon dates from enclosing metavolcanic rocks. The spread of $^{207}Pb/^{206}Pb$ dates obtained in our study from metasedimentary rock samples is relatively similar to that in the Bergslagen region.

6.5. Provenance and depositional setting

A great part of the nearly concordant $^{207}Pb/^{206}Pb$ dates from the apparent detrital zircon cores are within the age range of ca. 2.05–1.89 Ga, but this dataset also shows some older age peaks (the Palaeoproterozoic ones are shown in Fig. 5). These dates from SS 4 mostly include ≤2.02 Ga dates (Fig. 4e), but some of them may not record their original age (see subsection 6.2). The dates from SS 1, 3 and 5–7 show a prominent age peak at ca. 2.05–2.03 Ga (Fig. 5a–e). In addition, the most prominent age peak of these dates from type 1 grains of SS 4 (Fig. 5g) is at ca. 2.02 Ga. Thus, our dataset from apparent detrital zircon cores also indicates the prominent age peak at ca. 2.1–2.0 Ga. This is in accord with Huhma et al. (2011), who noted that detrital zircon data from most metasedimentary rocks in the Svecofennian province show a major peak at ca. 2.0 Ga.

In addition to the age peaks at 2.05–2.03 Ma, the nearly concordant datasets from the detrital zircon cores from the SS 5 (Häme migmatite suite) and SS 6–7 (Kimito suite) also show slightly younger, notable age peaks at ca. 2.00–1.99 Ga (Fig. 5c–e). Instead, age peaks at ca. 2.00–1.99 Ga are not equally prominent in the respective datasets from SS 1 and SS 3 (Häme migmatite suite). This difference in the age data may be simply explained e.g., by analytical errors or sampling bias but

interestingly, SS 5–7 are found within an area for which Nd isotopic data (Lahtinen & Huhma 1997; Rämö et al. 2001) suggest an older crustal component. In addition, the nearly concordant data from detrital cores include two >3.1 Ga $^{207}Pb/^{206}Pb$ dates, both of which were obtained from the area of this suggested older crustal component (one from SS 5 and one from SS 6).

In the case of each sampling site, there must have been multiple source areas for the zircons, or alternatively one provenance that already included older inherited zircons (see e.g., Huhma et al. 2011). Because of sedimentary recycling, it may not be possible to determine the ultimate source area of the rock (see e.g., Andersen et al. 2018a). Also, the sampling error may have an effect on the spread of the yielded dates (e.g., Fedo et al. 2003; Andersen et al. 2018a, 2018b).

All samples were also analysed for geochemical composition, and that geochemical data was used to provide implications for provenance and tectonic setting. We also used some samples from the Rock Geochemical Database of Finland (Rasilainen et al. 2007; see Fig. 1b for details and location of the selected samples) for comparison.

The provenances of the metasedimentary rocks were evaluated using a discrimination diagram based on Roser and Korch (1988) and a TiO_2/Zr diagram (fields according to Hayashi et al. 1997). The tectonic setting of the metasedimentary rocks, at the time of deposition, was estimated using discrimination diagrams based on Verma and Armstrong-Altrin (2013). These diagrams and more detailed examination of them are found in Appendix E. However, as such diagrams contain uncertainties due to e.g., recycling of sedimentary material, we consider them only as suggestive. The data of the geochemical database mostly plot similarly as our data in these diagrams (see Appendix E).

Based on the discrimination diagram for provenance and the TiO_2/Zr diagram, it seems that most of our samples and the samples of the Rock Geochemical Database would have had an intermediate or a felsic igneous provenance. The discrimination diagram suggests a more mafic provenance for the sample from SS 4, and this sample may actually have a mafic nature or a notable restite component.

In the discrimination diagrams for the tectonic setting, our samples and most of the samples of the Rock Geochemical Database plot in a rift or an arc field. Although these classifications are only indicative, they are still aligned with the earlier studies. Colley & Westra (1987) suggested that the western part of the Uusimaa belt (including the Kimito suite) formed in a volcanic–tectonic setting, where rifting occurred in a mature arc or continental crust. Väisänen & Mänttäri (2002) considered the volcanic rocks of the Orijärvi area in the Kisko group as volcanic arc and back arc rocks and suggested that the volcanic rocks east and west of the Orijärvi area were formed in a rift setting. Nironen (2017b) considered that the rocks in the upper part of the Kisko group were formed by rifting in a mature (continental) arc rather than back-arc.

7. Conclusions

Metasedimentary rock samples were collected from nine sampling sites in southern Finland. The following conclusions based the U-Pb zircon age results are presented:

- The obtained range of $^{207}Pb/^{206}Pb$ dates (3281–1810 Ma) is consistent with previously published data from Palaeoproterozoic metasedimentary rocks in the Svecofennian province in Finland. The nearly concordant dates from apparent detrital zircon cores indicate a prominent source with age around 2.1–2.0 Ga.
- The maximum depositional ages (MDAs) of sampling sites 1 and 3–7 span from 1.96 to 1.89 Ga thus slightly expanding the previously published MDA range within the study area. The defined MDAs suggest that the metasedimentary rocks in S-SW Finland are of approximately same age than in other parts of Svecofennian province in Finland.

- The obtained range of $^{207}Pb/^{206}Pb$ dates is consistent with the published $^{207}Pb/^{2067}Pb$ dates from the Bergslagen region in Sweden.
- The $^{207}Pb/^{206}Pb$ dates from zircon rims/overgrowths and metamorphic zircon grains suggest metamorphic events at least at ca. 1.89 and ca. 1.84 Ga and possibly also at ca. 1.87 Ga. The result is in accord with the documented regional metamorphic events of Svecofennian rocks in Finland.
- Some zircon rims and overgrowths yield ≥1.91 Ga $^{207}Pb/^{206}Pb$ dates. They mostly predate the estimated maximum depositional ages of the studied rocks and are possibly recording metamorphic events in their source areas.

Based on the metamorphic age of ca. 1.89 Ga and the previously published ages of the intrusive rocks, the minimum age of the deposition for the metasedimentary rocks is constrained to be ≤1.89 Ga. In addition, an intermediate dyke from the sampling site 3 yields an upper intercept age of 1846 ± 6 Ma, which provides an ultimate minimum age of deposition for the metasedimentary rock at this sampling site and possibly for all the studied metasedimentary rocks.

Acknowledgements

We thank Raimo Lahtinen for help with the field work and for his valuable comments on this manuscript. We also thank Seppo Töllikkö, Katariina Issukka, Leena Järvinen, Lasse Heikkinen and Jarmo Asikainen of the GTK laboratories for sample treatment, colleagues at GTK for advice concerning the petrographic examinations, and Hugh O'Brien for advice in analytical issues. We thank Mikko Nironen and Tom Andersen for the review of our manuscript, and Jarmo Kohonen for the editorial handling of the manuscript.

Supplementary Data

Electronic Appendices are available via Bulletin of the Geological Society Finland web page.

Electronic Appendix A: Description of the sampling sites, samples and zircons

Electronic Appendix B: Description of the analytical methods

Electronic Appendix C: Results of the geochemical analyses

Electronic Appendix D: U–Pb zircon age data

Electronic Appendix E: Geochemical characteristics: estimated provenance and tectonic setting of the studied samples.

References

Allen, R. L., Lundström, I., Ripa, M., Simeonov, A. & Christofferson, H., 1996. Facies Analysis of a 1.9 Ga, Continental Margin, Back-Arc, Felsic Caldera Province with Diverse Zn-Pb-Ag-(Cu-Au) Sulfide and Fe Oxide Deposits, Bergslagen Region, Sweden. Economic Geology, 91, 979–1008. https://doi.org/10.2113/gsecongeo.91.6.979

Alviola, R., Mänttäri, I., Mäkitie, H. & Vaasjoki, M., 2001. Svecofennian rare-element granitic pegmatites of the Ostrobothnia region, western Finland: their metamorphic environment and time of intrusion. In: Mäkitie, H. (ed.), Svecofennian granitic pegmatites (1.86-1.79 Ga) and quartz monzonite (1.87 Ga), and their metamorphic environment in the Seinäjoki region, western Finland. Geological Survey of Finland, Special Paper 30, pp. 9–29.

Andersen, T., 2005. Detrital zircons as tracers of sedimentary provenance: limiting conditions from statistics and numerical simulations. Chemical Geology 216, 249–270. https://doi.org/10.1016/j.chemgeo.2004.11.013

Andersen, T., Elburg, M.A. & Magwaza, B.N., 2019. Sources of bias in detrital zircon geochronology: Discordance, concealed lead loss and common lead correction. Earth-Science Reviews 197, 102899. https://doi.org/10.1016/j.earscirev.2019.102899

Andersen, T., Elburg, M.A., van Niekerk, H.S. & Ueckermann, H., 2018a. Successive sedimentary recycling regimes in southwestern Gondwana: Evidence from detrital zircons in Neoproterozoic to Cambrian sedimentary rocks in southern Africa. Earth-Science Reviews 181, 43–60. https://doi.org/10.1016/j.earscirev.2018.04.001

Andersen, T., Kristoffersen, M. & Elburg M.A., 2018b. Visualizing, interpreting and comparing detrital zircon age and Hf isotope data in basin analysis – a graphical approach. Basin Research 30, 132–147. https://doi.org/10.1111/bre.12245

Bedrock of Finland scale free, 2022. Digital Map Database [Electronic Resource] (Referred in 19.12.2022). Geological Survey of Finland (GTK). Online-address: http://hakku.gtk.fi

Bergman, S., Högdahl, K., Nironen, M., Ogenhall, E., Sjöström, H., Lundqvist, L. & Lahtinen, R., 2008. Timing of Palaeoproterozoic intra-orogenic sedimentation in the central Fennoscandian Shield; evidence from detrital zircon in metasandstone. Precambrian Research 161, 231–249. https://doi.org/10.1016/j.precamres.2007.08.007

Claesson, S., Huhma, H., Kinny, P.D. & Williams, I.S., 1993. Svecofennian detrital zircon ages— implications for the Precambrian evolution of the Baltic Shield. Precambrian Research 64, 109–130. https://doi.org/10.1016/0301-9268(93)90071-9

Colley, H. & Westra, L., 1987. The volcano-tectonic setting and mineralization of the early Proterozoic Kemiö-Orijärvi-Lohja belt, SW Finland. In: Pharaoh, T.C. et al. (eds.), Geochemistry and Mineralization of Proterozoic Volcanic Suites, Geological Society Special Publication 33, pp. 95–107. https://doi.org/10.1144/GSL.SP.1987.033.01.08

Coutts, D.S., Matthews, W.A. & Hubbard, S.P., 2019. Assessment of widely used methods to derive depositional ages from detrital zircon populations. Geoscience Frontiers 10, 1421–1435. https://doi.org/10.1016/j.gsf.2018.11.002

Dhuime, B., Bosch, D., Bruguier, O., Caby, R. & Pourtales, S., 2007. Age, provenance and post-deposition metamorphic overprint of detrital zircons from the Nathorst Land group (NE Greenland)—A LA-ICP-MS and SIMS study. Precambrian Research 155, 24–46. https://doi.org/10.1016/j.precamres.2007.01.002

Ehlers, C., Lindroos, A. & Selonen, O., 1993. The late Svecofennian granite-migmatite zone of southern Finland—a belt of transpressive deformation and granite emplacement. Precambrian Research 64, 295–309. https://doi.org/10.1016/0301-9268(93)90083-E

Fedo, C.M., Sircombe, K.N. & Rainbird, R.H., 2003. Detrital Zircon Analysis of the Sedimentary Record. In: Hanchar, J.M. & Hoskin, P.W.O. (eds.), Zircon, Reviews in Mineralogy and Geochemistry, vol. 53, pp. 277–303. https://doi.org/10.2113/0530277

Hayashi, K.-I., Fujisawa, H., Holland, H.D. & Ohmoto, H., 1997. Geochemistry of ~1.9 Ga sedimentary rocks from northeastern Labrador, Canada. Geochimica et Cosmochimica Acta 61, 4115–4137. https://doi.org/10.1016/S0016-7037(97)00214-7

Hopgood, A.M., Bowes, D.R., Kouvo, O. & Halliday, A.N., 1983. U-Pb and Rb-Sr Isotopic Study of Polyphase Deformed Migmatites in the Svecokarelides, Southern Finland. In: Atherton, M. & Gribble, C.D. (eds.), Migmatites, Melting and Metamorphism. Shiva Publishing Limited, Nantwich, pp. 80–92.

Huhma, H., 1986. Sm-Nd, U-Pb and Pb-Pb isotopic evidence for the origin of the Early Proterozoic Svecokarelian crust in Finland. Geological Survey of Finland, Bulletin 337, 48 p.

Huhma, H., Claesson, S., Kinny, P.D. & Williams, I.S., 1991. The growth of Early Proterozoic crust: new evidence from Svecofennian zircons. Terra Nova 3, 175–179. https://doi.org/10.1111/j.1365-3121.1991.tb00870.x

Huhma, H., O'Brien, H., Lahaye, Y. & Mänttäri, I., 2011. Isotope geology and Fennoscandian lithosphere evolution. In: Nenonen, K., & Nurmi, P.A. (eds.), Geoscience for Society: 125th Anniversary Volume. Geological Survey of Finland, Special Paper 49, pp. 35–48.

Hölttä, P. & Heilimo, E., 2017. Metamorphic map of Finland. In: Nironen, M. (ed.), Bedrock of Finland at the scale 1:1000 000 – Major stratigraphic units, metamorphism and tectonic evolution. Geological Survey of Finland, Special Paper 60, pp. 77–128.

Hölttä, P., Huhma, H., Lahaye, Y., Mänttäri, I., Lukkari, S. & O'Brien, H., 2019. Paleoproterozoic metamorphism in the northern Fennoscandian Shield: age constraints revealed by monazite. International Geology Review 62, 360–387. https://doi.org/10.1080/00206814.2019.1611488

Johansson, Å., Bingen, B., Huhma, H., Waight, T., Vestergaard, R., Soesoo, A., Skridlaite, G., Krzeminska, E., Shumlyanskyy, L., Holland, M.E., Holm-Denoma, C., Teixeira, W., Faleiros, F.M., Ribeiro, B.V., Jacobs, J., Wang, C., Thomas, R.J., Macey, P.H., Kirkland, C.L., Hartnady, M.I.H., Eglington, B.M., Puetz, S.J. & Condie, K.G., 2022. A geochronological review of magmatism along the external margin of Columbia and in the Grenville-age orogens forming the core of Rodinia. Precambrian Research 371, 106463. https://doi.org/10.1016/j.precamres.2021.106463

Johansson, Å. & Stephens, M.B., 2017. Timing of magmatism and migmatization in the 2.0–1.8 Ga accretionary Svecokarelian orogen, south-central Sweden. International Journal of Earth Sciences (Geol Rundsch) 106, 783–810. https://doi.org/10.1007/s00531-016-1359-3

Kara, J., Leskelä, T., Väisänen, M., Skyttä, P., Lahaye, Y., Tiainen, M. & Leväniemi, H., 2021. Early Svecofennian rift-related magmatism: Geochemistry, U-Pb-Hf zircon isotope data and tectonic setting of the Au-hosting Uunimäki gabbro, SW Finland. Precambrian Research 364, 106364. https://doi.org/10.1016/j.precamres.2021.106364

Kara, J., Väisänen, M., Heinonen, J.S., Lahaye, Y., O'Brien, H. & Huhma, H., 2020. Tracing arclogites in the Paleoproterozoic Era – A shift from 1.88 Ga calc-alkaline to 1.86 Ga high-Nb and adakite-like magmatism in

central Fennoscandian Shield. Lithos 372–373, 105663. https://doi.org/10.1016/j.lithos.2020.105663

Kathol, B., Serre, S.H. & Thomsen, T.B., 2020. Bergslagen etapp 1. Provenance of Svecofennian sedimentary rocks in Bergslagen and surrounding areas. SGU-rapport 2020:22, 84 p.

Kohn, M.J. & Kelly, N.G., 2018. Petrology and Geochronology of Metamorphic Zircon. In: Moser, D.E. et al. (eds.), Microstructural Geochronology: Planetary Down to Atom Scale, Geophysical Monograph 232, First edition, pp. 35–61. https://doi.org/10.1002/9781119227250.ch2

Korsman, K., Hölttä, P., Hautala, T. & Wasenius, P., 1984. Metamorphism as an indicator of evolution and structure of the crusts in eastern Finland. Geological Survey of Finland, Bulletin 328, 40 p.

Korsman, K., Niemelä, R. & Wasenius, P., 1988. Multistage evolution of the Proterozoic crust in the Savo schist belt, eastern Finland. In: Korsman, K. (ed.), Tectono-metamorphic evolution of the Raahe–Ladoga zone. Geological Survey of Finland, Bulletin 343, pp. 89–96.

Kotilainen, A.K., Mänttäri, I., Kurhila, M., Hölttä, P. & Rämö, O.T., 2016. Evolution of a Palaeoproterozoic giant magmatic dome in the Finnish Svecofennian; new insights from U/Pb geochronology: Precambrian Research 272, 39–56. https://doi.org/10.1016/j.precamres.2015.10.023

Kouvo, O., & Tilton, G.R., 1966. Mineral ages from the Finish Precambrian. Journal of Geology 74, 421–442. https://doi.org/10.1086/627176

Kuipers, G., Beunk, F.F., Yi, K. & van der Wateren, F.M., 2018. The Palaeoproterozoic Grythyttan Field in the Svecofennian Orogen, West Bergslagen, Central Sweden: structure, stratigraphy and age. Norwegian Journal of Geology 98, 333–357. https://dx.doi.org/10.17850/njg98-3-05

Kurhila, M., Mänttäri, I., Vaasjoki, M., Rämö, O.T. & Nironen, M., 2011. U-Pb geochronological constraints of the late Svecofennian leucogranites of southern Finland. Precambrian Research 190, 1–24. https://doi.org/10.1016/j.precamres.2011.07.008

Kurhila, M., Vaasjoki, M., Mänttäri, I., Rämö, O.T. & Nironen, M., 2005. U-Pb ages and Nd isotope characteristics of the lateorogenic, migmatizing microcline granites in southwestern Finland. Bulletin of the Geological Society of Finland 77, 105–128. https://doi.org/10.17741/bgsf/77.2.002

Kähkönen, Y. & Huhma, H., 1993. An Archaen cobble in a Svecofennian conglomerate near Tampere, southern Finland. In: Autio, S. (ed.), Geological Survey of Finland, Current Research 1991–1992. Geological Survey of Finland, Special Paper 18, pp. 31–36.

Lahtinen, R. & Huhma, H., 1997. Isotopic and geochemical constraints on the evolution of the 1.93-1.79 Ga Svecofennian crust and mantle in Finland. Precambrian Research 82, 13–34. https://doi.org/10.1016/S0301-9268(96)00062-9

Lahtinen, R., Huhma, H. & Kousa, J., 2002. Contrasting source components of the Paleoproterozoic Svecofennian metasediments: Detrital zircon U–Pb, Sm–Nd and geochemical data. Precambrian Research 116, 81–109. https://doi.org/10.1016/S0301-9268(02)00018-9

Lahtinen, R., Huhma, H., Kähkönen, Y. & Mänttäri, I., 2009. Paleoproterozoic sediment recycling during multiphase orogenic evolution in Fennoscandia, the Tampere and Pirkanmaa belts, Finland. Precambrian Research 174, 310–336. https://doi.org/10.1016/j.precamres.2009.08.008

Lahtinen, R., Huhma, H., Lahaye, Y., Kousa, J. & Luukas, J., 2015. Archean–Proterozoic collision boundary in central Fennoscandia; Revisited. Precambrian Research 261, 127–165. https://doi.org/10.1016/j.precamres.2015.02.012

Lahtinen, R., Huhma, H., Sipilä, P. & Vaarma, M., 2017. Geochemistry, U-Pb geochronology and Sm-Nd data from the Paleoproterozoic Western Finland supersuite – A key component in the coupled Bothnian oroclines. Precambrian Research 299, 264–281. https://doi.org/10.1016/j.precamres.2017.07.025

Lahtinen, R., Korja, A. & Nironen, M., 2005. Palaeoproterozoic tectonic evolution of the Fennoscandian Shield. In: Lehtinen, M. et al. (eds.), Precambrian Geology of Finland – Key to the evolution of the Fennoscandian Shield. Developments In Precambrian Geology, Elsevier Science B.V, pp. 481–532. https://doi.org/10.1016/S0166-2635(05)80012-X

Lahtinen, R., Salminen, P.E., Sayab, M., Huhma, H., Kurhila, M. & Johnston, S.T., 2022. Age and structural constraints on the tectonic evolution of the Paleoproterozoic Saimaa orocline in Fennoscandia. Precambrian Research 369, 106477. https://doi.org/10.1016/j.precamres.2021.106477

Ludwig, K.R., 2012. User's Manual for Isoplot 3.75–4.15. A Geochronological Toolkit for Microsoft Excel. Berkeley Geochronology Center, Special Publication 5, 1-75.

Luukas, J. & Kohonen, J., 2021. Major thrusts and thrust-bounded geological units in Finland: a tectonostratigraphic approach. In: Kohonen, J. & Tarvainen, T. (eds.), Developments in map data management and geological unit nomenclature in Finland. Geological Survey of Finland, Bulletin 412, pp. 81–114.

Matisto, A., 1968. Die Meta-arkose von Mauri bei Tampere. Bulletin de la Commission Géologique de Finland 235, 21 p. (In German with Finnish summary).

Mezger, K., Krogstad, J., 1997. Interpretation of discordant U-Pb zircon ages: An evaluation. Journal of Metamorphic Geology 15, 127–140. https://doi.org/10.1111/j.1525-1314.1997.00008.x

Mikkola, P., Heilimo, H., Luukas, J., Kousa, J., Aatos, S., Makkonen, H., Niemi, S., Nousiainen, M., Ahven, M., Romu, I. & Hokka, J., 2018a. Geological evolution and structure along the southeastern border of the Central Finland Granitoid Complex. In: Mikkola, P. et al. (eds.), Development of the Paleoproterozoic Svecofennian orogeny: new constraints from the southeastern boundary of the Central Finland Granitoid Complex. Geological Survey of Finland, Bulletin 407, pp. 5–27.

Mikkola, P., Huhma, H., Romu, I. & Kousa, J., 2018b. Detrital zircon ages and geochemistry of the metasedimentary rocks along the southeastern boundary of the Central Finland Granitoid Complex. In: Mikkola, P. et al. (eds.), Development of the Paleoproterozoic Svecofennian orogeny: new constraints from the southeastern boundary of the Central Finland Granitoid Complex. Geological Survey of Finland, Bulletin 407, pp. 28–55.

Mikkola, P., Mönkäre, K., Ahven, M. & Huhma, H., 2018c. Geochemistry and age of the Paleoproterozoic Makkola suite volcanic rocks in central Finland. In: Mikkola, P. et al. (eds.), Development of the Paleoproterozoic Svecofennian orogeny: new constraints from the southeastern boundary of the Central Finland Granitoid Complex. Geological Survey of Finland, Bulletin 407, pp. 85–105.

Mouri, H., Korsman, K. & Huhma, H., 1999. Tectono-metamorphic evolution and timing of the melting processes in the Svecofennian Tonalite-Trondhjemite Migmatite Belt: An example from Luopioinen, Tampere area, southern Finland. Bulletin of the Geological Society of Finland 71, 31–56. https://doi.org/10.17741/bgsf/71.1.003

Mouri, H., Väisänen, M., Huhma, H. & Korsman, K., 2005. Sm–Nd garnet and U–Pb monazite dating of high-grade metamorphism and crustal melting in the West Uusimaa area, southern Finland. GFF 127, 123–128. https://doi.org/10.1080/11035890501272123

Nelson, D.R., 2001. An assessment of the determination of depositional ages for precambrian clastic sedimentary rocks by U–Pb dating of detrital zircons. Sedimentary Geology 141–142, 37–60. https://doi.org/10.1016/S0037-0738(01)00067-7

Nironen, M., 1989. Emplacement and structural setting of granitoids in the early Proterozoic Tampere and Savo Schist Belts, Finland – implications for contrasting crustal evolution. Geological Survey of Finland, Bulletin 346, 83 p.

Nironen, M., 2017a. Guide to the Geological Map of Finland – Bedrock 1:1000 000. In: Nironen, M. (ed.), Bedrock of Finland at the scale 1:1000 000 – Major stratigraphic units, metamorphism and tectonic evolution. Geological Survey of Finland, Special Paper 60, pp. 41–76.

Nironen, M., 2017b. The Salittu Formation in southwestern Finland, part II: Picritic-basaltic volcanism in mature arch environment. Bulletin of the Geological Society of Finland 89, 5–19. https://doi.org/10.17741/bgsf/89.1.001

Nironen, M. & Mänttäri, I., 2012. Timing of accretion, intra-orogenic sedimentation and basin inversion in the Paleoproterozoic Svecofennian orogen: The Pyhäntaka area, southern Finland. Precambrian Research 192–195, 34–51. https://doi.org/10.1016/j.precamres.2011.09.013

Nironen, M., Mänttäri, I. & Väisänen, M., 2016. The Salittu Formation in southwestern Finland, part I: Structure, age and stratigraphy. Bulletin of the Geological Society of Finland 88, 85–103. https://doi.org/10.17741/bgsf/88.2.003

Pajunen, M., Hopgood, A., Huhma, H. & Koistinen, T., 2008. Integrated structural succession and age constraints on a Svecofennian key outcrop in Västerviken, southern Finland. In: Pajunen, M. (ed.), Tectonic evolution of the Svecofennian crust in southern Finland – a basis for characterizing bedrock technical properties. Geological Survey of Finland, Special Paper 47, pp. 161–184.

Patchett, J. & Kouvo, O., 1986. Origin of continental crust of 1.9-1.7 Ga age: Nd isotopes and U-Pb zircon ages in the Svecokarelian terrain of South Finland. Contributions to Mineralogy and Petrology 92, 1–12. https://doi.org/10.1007/BF00373959

Piazolo, S., Belousova, E., La Fontaine, A., Corcoran, C. & Cairney, J.M., 2017. Trace element homogeneity from micron- to atomic scale: Implication for the suitability of the zircon GJ-1 as a trace element reference material. Chemical Geology 456, 10–18. https://doi.org/10.1016/j.chemgeo.2017.03.001

Rasilainen, K., Lahtinen, R. & Bornhorst, T.J., 2007. The Rock Geochemical Database of Finland Manual. Geological Survey of Finland, Report of Investigation 164, 38 p.

Rasmussen, R., 2005. Zircon growth in very low grade metasedimentary rocks: evidence for zirconium mobility at ~250°C. Contributions to Mineralogy and Petrology 150, 146–155. http://dx.doi.org/10.1007/s00410-005-0006-y

Reinikainen, J., 2001. Petrogenesis of Paleoproterozoic marbles in the Svecofennian domain, Finland. Geological Survey of Finland, Report of Investigation 154, 84 p.

Roser, B.P. & Korsch, R.J., 1988. Provenance signatures of sandstone-mudstone suites determined using discriminant function analysis of major-element data. Chemical Geology 67, 119–139. https://doi.org/10.1016/0009-2541(88)90010-1

Rutland, R.W.R, Williams, I.S. & Korsman, K., 2004. Pre-1.91 Ga deformation and metamorphism in the Palaeoproterozoic Vammala Migmatite Belt, southern Finland, and implications for Svecofennian tectonics. Bulletin of the Geological Society of Finland 76, 93–140. https://doi.org/10.17741/bgsf/76.1-2.005

Rämö, O.T., Vaasjoki, M., Mänttäri, I., Elliott, B.A. & Nironen, M., 2001. Petrogenesis of the Post-kinematic Magmatism of the Central Finland Granitoid Complex I; Radiogenic Isotope Constraints and Implications for Crustal Evolution. Journal of Petrology 42, 1971–1993. https://doi.org/10.1093/petrology/42.11.1971

Salminen, P.E., Hölttä, P., Lahtinen, R. & Sayab, M., 2022. Monazite record for the Paleoproterozoic Svecofennian orogeny, SE Finland: An over 150-Ma spread of monazite dates. Lithos 416–417, 106654. https://doi.org/10.1016/j.lithos.2022.106654

Silva, J.P.A., Lana, C., Mazoz, A., Buick, I. & Scholz, R., 2023. U-Pb Saturn: New U-Pb/Pb-Pb Data Reduction Software for LA-ICP-MS. Geostandards and Geoanalytical Research, 49–66. https://doi.org/10.1111/ggr.12474

Skyttä, P., Käpyaho, A. & Mänttäri, I., 2005. Supracrustal rocks in the Kuovila area, Southern Finland: structural evolution, geochemical characteristics and the age of volcanism. Bulletin of the Geological Society of Finland 77, 129–150. https://doi.org/10.17741/bgsf/77.2.003

Skyttä, P. & Mänttäri, I., 2008. Structural setting of late Svecofennian granites and pegmatites in Uusimaa Belt, SW Finland: Age constraints and implications for crustal evolution. Precambrian Research 164, 86–109. https://doi.org/10.1016/j.precamres.2008.04.001

Spencer, C.J., Kirkland, C. & Taylor, R.J.M. 2016. Strategies towards statistically robust interpretations of *in situ* U–Pb zircon geochronology. Geoscience Frontiers 7, 581–589. https://doi.org/10.1016/j.gsf.2015.11.006

Stephens, M.B. & Andersson, J., 2015. Migmatization related to mafic underplating and intra- or back-arc spreading above a subduction boundary in a 2.0–1.8 Ga accretionary orogen, Sweden. Precambrian Research 264, 235–257. https://doi.org/10.1016/j.precamres.2015.04.019

Stephens, M.B., Ripa, M., Lundström, I., Persson, L., Bergman, T., Ahl, M., Wahlgren, C.-H., Persson, P.-O. & Wickström, L., 2009. Synthesis of the bedrock geology in the Bergslagen region, Fennoscandian Shield, south-central Sweden. Sveriges Geologiska Undersökning, Serie Ba 58, 259 p.

Suikkanen, E., Huhma, H., Kurhila, M. & Lahaye, Y., 2014. The age and origin of the Vaasa migmatite complex revisited. Bulletin of the Geological Society of Finland 86, 41–55. https://doi.org/10.17741/bgsf/86.1.003

Torvela, R. & Kurhila, M., 2022. Timing of syn-orogenic, high-grade transtensional shear zone formation in the West Uusimaa Complex, Finland. Bulletin of the Geological Society of Finland 94, 5–22. https://doi.org/10.17741/bgsf/94.1.001

Vaasjoki, M. & Sakko, M., 1988. The evolution of the Raahe-Ladoga zone in Finland: isotopic composition. In: Korsman, K. (ed.), Tectono-metamorphic evolution of the Raahe–Ladoga zone. Geological Survey of Finland, Bulletin 343, pp. 7–32.

Van Duin, J.A., 1992. The Turku granulite area, SW Finland: a fluid-absent Svecofennian granulite occurrence. Dissertation, Vrije Universiteit, Amsterdam, 234 p.

Verma, S.P. & Armstrong-Altrin, J.S., 2013. New multi-dimensional diagrams for tectonic discrimination of siliciclastic sediments and their application to Precambrian basins. Chemical Geology 355, 117–133. https://doi.org/10.1016/j.chemgeo.2013.07.014

Vermeesch, P., 2021. Maximum depositional age estimation revisited. Geoscience Frontiers 12, 843–850. https://doi.org/10.1016/j.gsf.2020.08.008

Väisänen, M. & Kirkland, C. L., 2008. U-Th-Pb zircon geochronology on igneous rocks in the Toija and Salittu Formations, Orijärvi area, southwestern Finland: constraints on the age of volcanism and metamorphism. Bulletin of the Geological Society of Finland 80, 73–87. https://doi.org/10.17741/bgsf/80.2.001

Väisänen, M. & Mänttäri, I., 2002. 1.90-1.88 Ga arc and back-arc basin in the Orijärvi area, SW Finland. Bulletin of the Geological Society of Finland 74, 185–214. https://doi.org/10.17741/bgsf/74.1-2.009

Väisänen, M., Mänttäri, I. & Hölttä, P., 2002. Svecofennian magmatic and metamorphic evolution in southwestern Finland as revealed by U-Pb zircon SIMS geochronology. Precambrian Research 116, 111–127. https://doi.org/10.1016/S0301-9268(02)00019-0

Williams, I., S., Rutland, R.W.R. & Kousa, J., 2008. A regional 1.92 Ga tectonothermal episode in Ostrobothnia, Finland: Implications for models of Svecofennian accretion. Precambrian Research 165, 15–36. https://doi.org/10.1016/j.precamres.2008.05.004

Zimmerman, S., Mark, C., Chew, D. & Voice, P.J., 2018. Maximising data and precision from detrital zircon U-Pb analysis by LA-ICPMS: The use of core-rim ages and the single-analysis concordia age. Sedimentary Geology 375, 5–13. https://doi.org/10.1016/j.sedgeo.2017.12.020